Wiener model identification and predictive control of a pH neutralisation process

J.C. Gómez, A. Jutan and E. Baeyens

Abstract: Wiener model identification and predictive control of a pH neutralisation process is presented. Input-output data from a nonlinear, first principles simulation model of the pH neutralisation process are used for subspace-based identification of a black-box Wiener-type model. The proposed nonlinear subspace identification method has the advantage of delivering a Wiener model in a format which is suitable for its use in a standard linear-model-based predictive control scheme. The identified Wiener model is used as the internal model in a model predictive controller (MPC) which is used to control the nonlinear white-box simulation model. To account for the unmeasurable disturbance, a nonlinear observer is proposed. The performance of the Wiener model predictive control (WMPC) is compared with that of a linear MPC, and with a more traditional feedback control, namely a PID control. Simulation results show that the WMPC outperforms the linear MPC and the PID controllers.

1 Introduction

The control of pH processes is a problem frequently encountered in the chemical process and biotechnology industries. It has been recognised as a challenging problem due to the time-varying and nonlinear characteristics of the pH processes. This is particularly true when control has to be achieved in the neutral range (a pH between six and eight) when only strong acids and strong bases are present. Several techniques have been proposed in the literature for the control of pH processes, most of them resorting to nonlinear adaptive schemes. For instance, [1] and [2], have proposed and experimentally evaluated an adaptive nonlinear controller which is the combination of an input-output linearising controller and a reduced-order, open-loop, nonlinear observer for the estimation of the unmeasurable disturbance (the buffer flow rate). Narayanan *et al.* [3] have proposed an adaptive nonlinear internal model control, which combines the concepts of nonlinear internal model control, strong acid equivalent (introduced in [4]) and adaptive mechanisms.

Some research has also been conducted on model predictive control (MPC) of pH processes. MPC refers to a class of control algorithms in which a dynamic process model is used to predict and optimise process performance (see, for instance, the recent book by Maciejowski [5]). MPC has been used in industry for more than 30 years, and has become an industry standard mainly due to its intrinsic capability for dealing with constraints (often, a most efficient (and profitable) operation requires the process to work at or near such constraints) and with multivariable systems. Most commercially available MPC technologies are based on a linear model of the process. For processes which are highly nonlinear, the performance of an MPC based on a linear model can be poor. This has motivated the development of nonlinear model predictive control (NMPC), where a more accurate (nonlinear) model of the plant is used for prediction and optimisation (see for instance [6] for a survey on the current status and future directions of NMPC).

Many of the current NMPC schemes are based on physical models of the process. However, in many cases such models are difficult to derive, and are often not available at all. In these cases it makes sense to use a nonlinear empirical model, identified from input-output measurements. Some works where this approach has been followed are for instance: [7] where a nonlinear predictive control scheme based on radial basis functions models is proposed, [8] and [9] where the NMPC is based on a Hammerstein model, and [9–11], where the NMPC is based on a Wiener model. In all these works the paradigmatic application has been pH neutralisation processes.

From an identification point of view, pH processes have often been considered in the literature as having a Wiener structure (see for instance [12]) consisting of the cascade connection of a linear time-invariant (LTI) system followed by a static (memoryless) nonlinearity. In this structure, the linear block represents the mixing dynamics of the reagent streams in the continous stirred tank reactor, while the static nonlinearity represents the nonlinear titration curve which gives the pH of the effluent solution as a function of the chemical components.

Wiener models have the capability of approximating, with arbitrary accuracy, any fading memory nonlinear time-invariant system [13], and they have been successfully used to model several nonlinear systems encountered in the

© IEE, 2004

IEE Proceedings online no. 20040438

doi: 10.1049/ip-cta:20040438

Paper first received 27th August 2003 and in revised form 21st January 2004

J.C. Gómez is with the Laboratory for System Dynamics and Signal Processing, FCEIA, Universidad Nacional de Rosario, Riobamba, 245 Bis, 2000 Rosario, Argentina

A. Jutan is with the Department of Chemical and Biochemical Engineering, The University of Western Ontario, London, ON, Canada, N6A 5B9

E. Baeyens is with the Department of Systems Engineering and Automatic Control, ETSII, Universidad de Valladolid, Paseo del Cauce s/n, 47011 Valladolid, Spain

process industry, such as distillation columns [14], and pH processes [10–12].

Several methods have been proposed in the literature for the identification of Wiener models (see for instance [15–17], for some classical identification methods for Wiener models). More recently, some research interest has been focused on extending linear subspace identification methods [18–20], for this class of nonlinear models (see [21–23] for subspace identification of Hammerstein and Wiener models).

The subspace method introduced in [23] by the first and the third authors will now be used to identify a Wiener model from input-output data generated from a nonlinear first principles simulation model of the pH neutralisation process. This identified Wiener model is in turn used in a model predictive controller. It is shown that the structure of the identified Wiener model is suitable for its use in a standard (based on a linear model) MPC strategy, therefore preserving the stability and numerical properties of the involved algorithms. In contrast to similar approaches to Wiener model predictive control (WMPC) in the literature (see for instance [9–11]), there is no need to invert the static nonlinearity, since it is the inverse of the nonlinearity which is delivered by the identification algorithm proposed here. In particular, if a quadratic criterion and linear constraints are chosen, the optimisation problem involved in the WMPC scheme proposed remains a highly convex quadratic program (QP) problem, which can be solved efficiently resorting to existing algorithms. In order to compensate for the unmeasurable disturbance (the buffer flow rate), a nonlinear observer based on a white-box simulation model is proposed and used as a soft sensor in the WMPC scheme. For the purposes of comparison, the same input-output data used for the identification of the Wiener model are used to identify a linear model using subspace methods. A model predictive controller is implemented based on this model, and its performance is compared to that of the NMPC based on the Wiener model. Also for the purposes of comparison, a standard PID controller is implemented on the process.

2 Process description

The considered pH neutralisation process consists of an acid (HNO_3) stream, a base (NaOH) stream, and a buffer ($NaHCO_3$) stream that are mixed in a constant volume (V) stirring tank. The process is schematically depicted in Fig. 1, and corresponds to a bench-scale plant at UCSB (see [1, 2]).

The inputs to the system are the base (volumetric) flow rate (u_1), the buffer flow rate (u_2) and the acid flow rate (u_3), while the output (y) is the pH of the effluent solution. The acid flow rate (u_3), as well as the volume (V) of the tank are assumed to be constant. Usually, the objective is to control the pH of the effluent solution by manipulating the base flow rate, despite the variations of the unmeasured buffer flow rate, which can be considered as a disturbance.

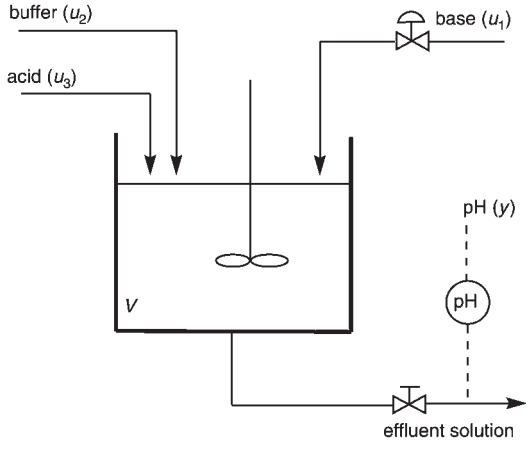

Fig. 1 *Schematic representation of the pH neutralisation process*

Table 1: Nominal operating conditions

$u_3 = 16.60$ ml/s	$u_2 = 0.55$ ml/s
$u_1 = 15.55$ ml/s	$V = 2900$ ml
$W_{a1} = -3.05 \times 10^{-3}$ mol	$W_{a2} = -3 \times 10^{-2}$ mol
$W_{a3} = 3 \times 10^{-3}$ mol	$W_a = -4.32 \times 10^{-4}$ mol
$W_{b1} = 5 \times 10^{-5}$ mol	$W_{b2} = 3 \times 10^{-2}$ mol
$W_{b3} = 0$ mol	$W_b = 5.28 \times 10^{-4}$ mol
$pK_1 = 6.35$	$pK_2 = 10.25$
$y = 7.0$	

A simulation model, based on first principles, was presented in [1] introducing two reaction invariants (one related to a charge balance and the other to a balance on the carbonate ion) for each inlet/outlet stream. The reaction invariants will be denoted here as (W_{a1}, W_{b1}), (W_{a2}, W_{b2}), (W_{a3}, W_{b3}), and (W_a, W_b), for the base stream, the buffer stream, the acid stream and the effluent solution respectively. The model is highly nonlinear due to the implicit output equation, known as the titration curve (7). The dynamic model for the reaction invariants of the effluent solution (W_a, W_b), in state-space form, is given by [1, 2]:

$$\dot{\boldsymbol{x}} = \boldsymbol{f}(\boldsymbol{x}) + \boldsymbol{g}(\boldsymbol{x})u_1 + \boldsymbol{p}(\boldsymbol{x})u_2 \tag{1}$$

$$h(\boldsymbol{x}, y) = 0 \tag{2}$$

where

$$\boldsymbol{x} \stackrel{\Delta}{=} [x_1, x_2]^T = [W_a, W_b]^T \tag{3}$$

$$\boldsymbol{f}(\boldsymbol{x}) = \left[\frac{u_3}{V}(W_{a3} - x_1), \frac{u_3}{V}(W_{b3} - x_2)\right]^T \tag{4}$$

$$\boldsymbol{g}(\boldsymbol{x}) = \left[\frac{1}{V}(W_{a1} - x_1), \frac{1}{V}(W_{b1} - x_2)\right]^T \tag{5}$$

$$\boldsymbol{p}(\boldsymbol{x}) = \left[\frac{1}{V}(W_{a2} - x_1), \frac{1}{V}(W_{b2} - x_2)\right]^T \tag{6}$$

$$h(\boldsymbol{x}, y) = x_1 + 10^{y-14} - 10^{-y} + x_2 \frac{1 + 2 \times 10^{y-pK_2}}{1 + 10^{pK_1 - y} + 10^{y-pK_2}} \tag{7}$$

Here, the parameters pK_1 and pK_2 are the first and second disassociation constants of the weak acid H_2CO_3. The nominal operating conditions of the system are given in [1] and [2], and they are reproduced in Table 1 for the sake of completeness.

In order to compensate for the variations in the buffer flow rate (considered here as a disturbance), a nonlinear observer for its online estimation is proposed in Section 4.

3 Subspace-based Wiener model identification

For the sake of completeness, the subspace-based Wiener model identification method originally introduced by the first and third authors in [23] is summarised in this Section.

A (multivariable) Wiener model is schematically depicted in Fig. 2. The model consists of the cascade connection of an LTI system followed by a zero-memory

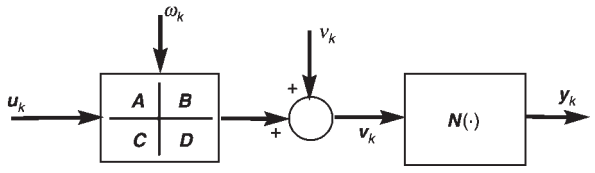

Fig. 2 *Multivariable Wiener model*

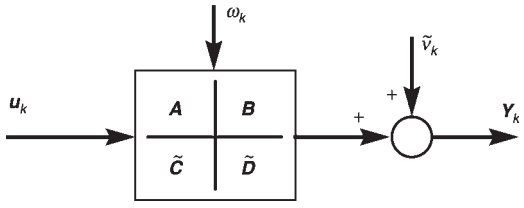

Fig. 3 *Equivalent LTI model*

nonlinear element with input-output characteristic given by $\boldsymbol{N}(\cdot)$. The LTI subsystem has a state-space representation of the form:

$$\boldsymbol{x}_{k+1} = \boldsymbol{A}\boldsymbol{x}_k + \boldsymbol{B}\boldsymbol{u}_k + \omega_k \tag{8}$$

$$\boldsymbol{v}_k = \boldsymbol{C}\boldsymbol{x}_k + \boldsymbol{D}\boldsymbol{u}_k + \nu_k \tag{9}$$

where $\boldsymbol{A}$, $\boldsymbol{B}$, $\boldsymbol{C}$ and $\boldsymbol{D}$, are the system matrices of appropriate dimensions, and where $\boldsymbol{x}_k \in \mathbb{R}^n$, $\boldsymbol{v}_k \in \mathbb{R}^m$, $\boldsymbol{u}_k \in \mathbb{R}^p$ and $\nu_k \in \mathbb{R}^m$, represent the LTI system state, output, input and process noise vectors at time k, respectively.

It is assumed that the static nonlinear function $\boldsymbol{N}(\cdot) : \mathbb{R}^m \rightarrow \mathbb{R}^m$ is invertible, and that its inverse $\boldsymbol{N}^{-1}(\cdot)$ can be described as a liner combination of basis functions in the form:

$$\boldsymbol{N}^{-1}(\boldsymbol{y}_k) = \sum_{i=1}^{r} \boldsymbol{\alpha}_i \boldsymbol{g}_i(\boldsymbol{y}_k) \tag{10}$$

where $\boldsymbol{g}_i(\cdot) : \mathbb{R}^m \rightarrow \mathbb{R}^m$, $(i = 1, \ldots, r)$, are the assumed known nonlinear basis functions, and $\boldsymbol{\alpha}_i \in \mathbb{R}^{m \times m}$, $(i = 1, \ldots, r)$, are unknown matrix parameters. Typically, the basis functions are polynomials (any smooth function in an interval can be represented with arbitrary accuracy by a polynomial of sufficiently high order) but they can also be basis functions generated by translations and dilations of a mother function (e.g. wavelets, or radial basis functions).

With this representation for the static nonlinearity, (9) can be written as,

$$\boldsymbol{\alpha}\boldsymbol{Y}_k \stackrel{\Delta}{=} \sum_{i=1}^{r} \boldsymbol{\alpha}_i \boldsymbol{g}_i(\boldsymbol{y}_k) = \boldsymbol{C}\boldsymbol{x}_k + \boldsymbol{D}\boldsymbol{u}_k + \nu_k \tag{11}$$

where $\boldsymbol{\alpha} \stackrel{\Delta}{=} [\boldsymbol{\alpha}_1, \cdots, \boldsymbol{\alpha}_r]$, $\boldsymbol{Y}_k \stackrel{\Delta}{=} [\boldsymbol{g}_1^T(\boldsymbol{y}_k), \cdots, \boldsymbol{g}_r^T(\boldsymbol{y}_k)]^T$. The Wiener model can then be described as:

$$\boldsymbol{x}_{k+1} = \boldsymbol{A}\boldsymbol{x}_k + \boldsymbol{B}\boldsymbol{u}_k + \omega_k \tag{12}$$

$$\boldsymbol{Y}_k = \tilde{\boldsymbol{C}}\boldsymbol{x}_k + \tilde{\boldsymbol{D}}\boldsymbol{u}_k + \tilde{\nu}_k, \tag{13}$$

with $\tilde{\boldsymbol{C}} \stackrel{\Delta}{=} \boldsymbol{\alpha}^\dagger \boldsymbol{C}, \tilde{\boldsymbol{D}} \stackrel{\Delta}{=} \boldsymbol{\alpha}^\dagger \boldsymbol{D}$, $\tilde{\nu}_k \stackrel{\Delta}{=} \boldsymbol{\alpha}^\dagger \nu_k$, and where $\boldsymbol{\alpha}^\dagger$ stands for the left pseudo-inverse of $\boldsymbol{\alpha}$. It can be seen from (12) and (13) that the parametrisation (8), (9) and (10) is not unique, since any parameter matrices $\boldsymbol{\beta}\boldsymbol{C}$, $\boldsymbol{\beta}\boldsymbol{D}$ and $\boldsymbol{\alpha}^\dagger\boldsymbol{\beta}^{-1}$, for some nonsingular matrix $\boldsymbol{\beta} \in \mathbb{R}^{m \times m}$, provide the same description as (12) and (13). To obtain a one-to-one parametrisation i.e. for the system to be identifiable, additional constraints must be imposed on the parameters. A technique that can be used to obtain uniqueness is to normalise the parameter matrices $\boldsymbol{\alpha}^\dagger$, that is to assume for instance that $\|\boldsymbol{\alpha}^\dagger\|_2 = 1$. Under this assumption the parametrisation of (8), (9) and (10) is unique.

Remark 1: Equations (12) and (13) can be interpreted as a state-space realisation of a LTI system whose output $\boldsymbol{Y}_k$ is a transformed (by the nonlinear and known basis functions $\boldsymbol{g}_i(\cdot)$) version of the original output $\boldsymbol{y}_k$. A block diagram representation of (12) and (13) is depicted in Fig. 3.

It is this equivalent LTI model that will be used as the internal model in a standard (based on a linear model) MPC strategy in Section 6. This, of course, is an additional advantage of the Proposed identification method, since it delivers a Wiener model in a format that can be used directly in a standard linear model-based MPC.

Based on this representation, any available subspace identification algorithm (such as the N4SID algorithm by Van Overschee and de Moor [18], the MOESP algorithm by Verhaegen [19], or the CVA algorithm by Larimore [20], can then be employed to obtain estimates of the system matrices $\boldsymbol{A}$, $\boldsymbol{B}$, $\tilde{\boldsymbol{C}}$ and $\tilde{\boldsymbol{D}}$ from input-output data.

Given the estimates $\hat{\boldsymbol{A}}$, $\hat{\boldsymbol{B}}$, $\hat{\tilde{\boldsymbol{C}}}$ and $\hat{\tilde{\boldsymbol{D}}}$ of the matrices $\boldsymbol{A}$, $\boldsymbol{B}$, $\tilde{\boldsymbol{C}}$ and $\tilde{\boldsymbol{D}}$, respectively, the problem is how to compute estimates of the matrices $\boldsymbol{C}$, $\boldsymbol{D}$ and $\boldsymbol{\alpha}$. Matrices $\tilde{\boldsymbol{C}}$ and $\tilde{\boldsymbol{D}}$ can be expressed in a combined form as:

$$[\tilde{\boldsymbol{C}}\tilde{\boldsymbol{D}}] = \boldsymbol{\alpha}^\dagger [\boldsymbol{C}\boldsymbol{D}] \tag{14}$$

The best (in the mean-squares sense) estimates of matrices $\boldsymbol{C}$, $\boldsymbol{D}$ and $\boldsymbol{\alpha}$ are such that:

$$(\hat{\boldsymbol{C}}, \hat{\boldsymbol{D}}, \hat{\boldsymbol{\alpha}}^\dagger) = \arg\min_{\boldsymbol{C}, \boldsymbol{D}, \boldsymbol{\alpha}^\dagger} \left\{ \left\| [\hat{\tilde{\boldsymbol{C}}} \quad \hat{\tilde{\boldsymbol{D}}}] - \alpha^\dagger [\boldsymbol{C} \quad \boldsymbol{D}] \right\|_2^2 \right\} \tag{15}$$

The solution to this minimisation problem is provided by the SVD of the matrix $[\hat{\tilde{\boldsymbol{C}}}\ \hat{\tilde{\boldsymbol{D}}}]$. The result is summarised in theorem 3.1 in [23]. Based on this result, the subspace identification algorithm for the Wiener model can be summarised as follows:

Algorithm 1:
Step 1: Compute estimates $(\hat{\boldsymbol{A}}, \hat{\boldsymbol{B}}, \hat{\tilde{\boldsymbol{C}}}, \hat{\tilde{\boldsymbol{D}}})$ of the systems matrices $(\boldsymbol{A}, \boldsymbol{B}, \tilde{\boldsymbol{C}}, \tilde{\boldsymbol{D}})$ in (12) and (13) using any available subspace algorithm for LTI systems.
Step 2: Compute the economy size SVD of $[\hat{\tilde{\boldsymbol{C}}} \quad \hat{\tilde{\boldsymbol{D}}}]$, and the partition of this decomposition as:

$$[\hat{\tilde{\boldsymbol{C}}} \quad \hat{\tilde{\boldsymbol{D}}}] = \boldsymbol{U}_s \boldsymbol{\Sigma}_s \boldsymbol{V}_s^T \stackrel{\Delta}{=} [\boldsymbol{U}_1 \quad \boldsymbol{U}_2] \begin{bmatrix} \boldsymbol{\Sigma}_1 & 0 \\ 0 & \boldsymbol{\Sigma}_2 \end{bmatrix} \begin{bmatrix} \boldsymbol{V}_1^T \\ \boldsymbol{V}_2^T \end{bmatrix} \tag{16}$$

where $\boldsymbol{\Sigma}_s$ is a diagonal matrix containing the s nonzero singular values $(\sigma_i, i = 1, \cdots, s)$ of $[\hat{\tilde{\boldsymbol{C}}} \quad \hat{\tilde{\boldsymbol{D}}}]$ in nonincreasing order, and where the unitary matrices $\boldsymbol{U}_s = [u_1\, u_2\, \cdots\, u_s] \in \mathbb{R}^{mr \times s}$ and $\boldsymbol{V}_s = [v_1\, v_2\, \cdots\, v_s] \in \mathbb{R}^{(n+p) \times s}$ contain the corresponding left and right singular vectors, respectively. The partition of the SVD in (16) is such that the following dimensions for the matrices $\boldsymbol{\Sigma}_1$, $\boldsymbol{U}_1$ and $\boldsymbol{V}_1$ hold, $\boldsymbol{\Sigma}_1 \in \mathbb{R}^{m \times m}$, $\boldsymbol{U}_1 \in \mathbb{R}^{mr \times m}$ and $\boldsymbol{V}_1 \in \mathbb{R}^{(n+p) \times m}$.
Step 3: Compute the estimates of the parameter matrices $\boldsymbol{C}$, $\boldsymbol{D}$ and $\boldsymbol{\alpha}$ as $[\hat{\boldsymbol{C}}\ \hat{\boldsymbol{D}}] = \boldsymbol{\Sigma}_1 \boldsymbol{V}_1^T$, and $\hat{\boldsymbol{\alpha}} = \boldsymbol{U}_1^\dagger$, respectively. □

4 Nonlinear observer

The nonlinear first principles model of (1) and (2) can be written as:

$$\dot{\boldsymbol{x}} = \boldsymbol{G}(\boldsymbol{x}, u_1) + \boldsymbol{F}(\boldsymbol{x})u_2 \tag{17}$$

$$h(\boldsymbol{x}, y) = 0 \tag{18}$$

with the obvious definitions for the functions $\boldsymbol{G}(\boldsymbol{x}, u_1)$ and $\boldsymbol{F}(\boldsymbol{x})$. In [24], a nonlinear observer for the estimation of the constant (slowly varying) parameter u_2 in a dynamic system of the form (17) has been proposed The nonlinear observer in [24] is described by:

$$\hat{\boldsymbol{u}}_2 = \phi(\boldsymbol{x}) + \xi \tag{19}$$

$$\dot{\xi} = -\boldsymbol{\Phi}(\boldsymbol{x})[\boldsymbol{G}(\boldsymbol{x}, u_1) + \boldsymbol{F}(\boldsymbol{x})\hat{\boldsymbol{u}}_2] \tag{20}$$

where $\hat{\boldsymbol{u}}_2$ is the estimated parameter, ξ is the observer state, $\phi(\boldsymbol{x})$ is an appropriately chosen nonlinear function, and $\boldsymbol{\Phi}(\boldsymbol{x})$ is its Jacobian matrix, i.e.:

$$\boldsymbol{\Phi}(\boldsymbol{x}) = \left[\frac{\partial \phi_i(\boldsymbol{x})}{\partial x_j}\right] \tag{21}$$

The matrix $\boldsymbol{\Phi}(\boldsymbol{x})$ (or equivalently $\phi(\boldsymbol{x})$) has to be chosen in such a way to ensure that the estimation error:

$$e \stackrel{\Delta}{=} u_2 - \hat{\boldsymbol{u}}_2 \tag{22}$$

converges to zero with the desired speed. Assuming the parameter u_2 is constant, the estimation error dynamics are given by:

$$\begin{aligned} \dot{e} &= -\dot{\hat{\boldsymbol{u}}}_2 \\ &= -\boldsymbol{\Phi}(\boldsymbol{x})\dot{\boldsymbol{x}} - \dot{\xi} \\ &= -\boldsymbol{\Phi}(\boldsymbol{x})\boldsymbol{F}(\boldsymbol{x})e \\ &= -\boldsymbol{L}(\boldsymbol{x})e \end{aligned} \tag{23}$$

with $\boldsymbol{L}(\boldsymbol{x}) \stackrel{\Delta}{=} \boldsymbol{\Phi}(\boldsymbol{x})\boldsymbol{F}(\boldsymbol{x})$. Notice that the estimation error dynamics are linear. However, since the matrix $\boldsymbol{L}(\boldsymbol{x})$ is time-varying, to ensure the asymptotic stability of (23) it is not sufficient to ask for the eigenvalues of $\boldsymbol{L}(\boldsymbol{x})$ to be in the open left half-plane. If $\boldsymbol{L}(\boldsymbol{x})$ can be chosen to be a positive semidefinite symmetric matrix, then resorting to Lyapunov theory and Barbalat's lemma (see lemma 1.2.1 and corollary 1.2.2 in [25]), a sufficient condition for the asymptotic convergence of the error to zero is that $\boldsymbol{L}(\boldsymbol{x})$ be bounded. A detailed proof is provided in the Appendix.

As pointed out in [24], one possible way (but not the only one) of selecting $\boldsymbol{\Phi}(\boldsymbol{x})$ such that $\boldsymbol{L}(\boldsymbol{x})$ is a positive semidefinite symmetric matrix is as:

$$\boldsymbol{\Phi}(\boldsymbol{x}) = \boldsymbol{F}^T(\boldsymbol{x})\boldsymbol{H} \tag{24}$$

where $\boldsymbol{H}$ is a positive definite constant matrix. Choosing $\boldsymbol{H} = k_{u_2}\boldsymbol{I}$, with $k_{u_2} > 0$ a positive constant, and $\boldsymbol{I}$ the identity matrix of appropriate dimensions, matrix $\boldsymbol{\Phi}(\boldsymbol{x})$ can be written as:

$$\boldsymbol{\Phi}(\boldsymbol{x}) = k_{u_2}\boldsymbol{F}^T(\boldsymbol{x}) = \frac{k_{u_2}}{V}[(W_{a2} - x_1), (W_{b2} - x_2)] \tag{25}$$

so that matrix $\phi(\boldsymbol{x})$ is given by:

$$\phi(\boldsymbol{x}) = -\frac{k_{u_2}}{2V}\left[(W_{a2} - x_1)^2 + (W_{b2} - x_2)^2\right] \tag{26}$$

Summarising, the asymptotic observer for the estimation of the disturbance (the buffer flow rate) is given by (19), (20), (25) and (26). The dynamic response of the observer can be adjusted by modifying the tuning parameter k_{u_2}.

The main drawback of the proposed nonlinear observer is the assumption that the full state vector is available for the estimation. For the case of the pH process, this assumption is unrealistic since the states (the reaction invariants of the effluent solution) are not measurable. To solve this problem, a state observer is proposed and the observed states are used instead of the actual, states in the disturbance observer (19), (20), (25) and (26). That is, the certainty equivalence principle is assumed to hold for the combined scheme. Although the assumption is true for linear system, this is not always the case when applied to nonlinear systems. The proposed state observer has a Luenberger-type structure of the form:

$$\dot{\hat{\boldsymbol{x}}} = \underbrace{\boldsymbol{G}(\hat{\boldsymbol{x}}, u_1) + \boldsymbol{F}(\hat{\boldsymbol{x}})u_2}_{\text{plant dynamics}} + \underbrace{\boldsymbol{K}(\hat{\boldsymbol{x}})(y - \hat{y})}_{\text{correction term}} \tag{27}$$

$$h(\hat{\boldsymbol{x}}, \hat{y}) = 0 \tag{28}$$

where $\hat{\boldsymbol{x}}$ is the observed state, $\hat{y}$ is the observed output and $\boldsymbol{K}(\hat{\boldsymbol{x}})$ is an appropriately chosen nonlinear function, usually, the observability matrix computed from the Lie derivatives of the output map along the vector field $\boldsymbol{f}(\hat{\boldsymbol{x}})$ (see [26]). Due to the implicit output equation (18), the observability matrix cannot be computed explicitly. An alternative for this is to choose:

$$\boldsymbol{K}(\hat{\boldsymbol{x}}) = k_x\boldsymbol{F}(\hat{\boldsymbol{x}}) \tag{29}$$

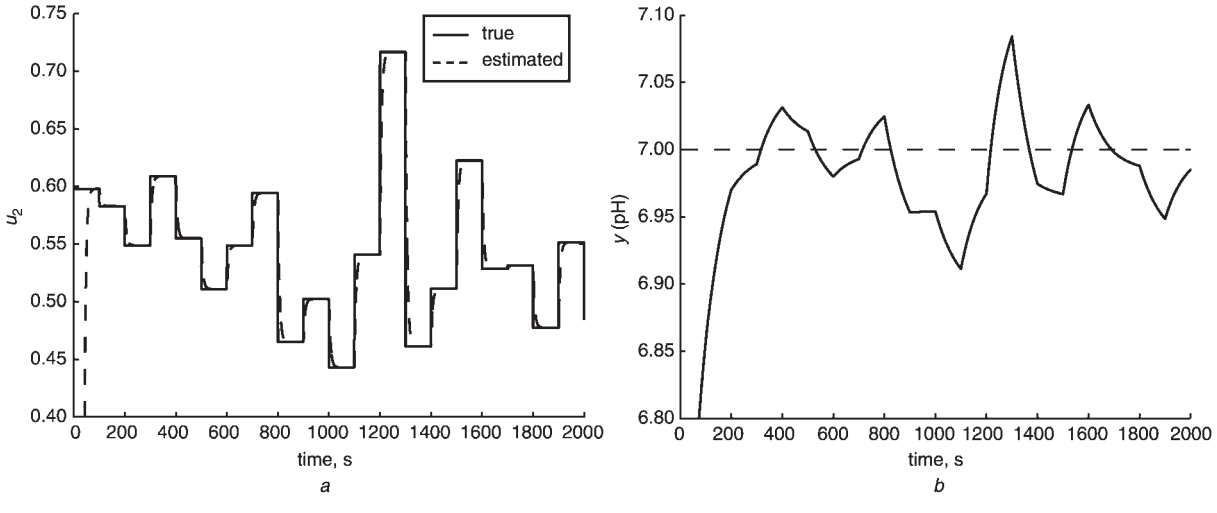

Fig. 4

a True and estimated disturbance (u_2)
b Output (pH)

which means that a correction term proportional to the output error is being added to the parameter u_2, since for this case (27) becomes:

$$\dot{\hat{\boldsymbol{x}}} = \boldsymbol{G}(\hat{\boldsymbol{x}}, u_1) + \boldsymbol{F}(\hat{\boldsymbol{x}}) \left[u_2 + \underbrace{k_x(y - \hat{y})}_{\text{correction term}} \right] \tag{30}$$

The combined observer scheme is then given by:

$$\hat{u}_2 = \phi(\hat{\boldsymbol{x}}) + \xi \tag{31}$$

$$\dot{\xi} = -\boldsymbol{\Phi}(\hat{\boldsymbol{x}})[\boldsymbol{G}(\hat{\boldsymbol{x}}, u_1) + \boldsymbol{F}(\hat{\boldsymbol{x}})\hat{u}_2] \tag{32}$$

$$\dot{\hat{\boldsymbol{x}}} = \boldsymbol{G}(\hat{\boldsymbol{x}}, u_1) + \boldsymbol{F}(\hat{\boldsymbol{x}})[\hat{u}_2 + k_x(y - \hat{y})] \tag{33}$$

$$h(\hat{\boldsymbol{x}}, \hat{y}) = 0 \tag{34}$$

with $\boldsymbol{\Phi}(\boldsymbol{x})$ and $\phi(\boldsymbol{x})$ as in (25) and (26), respectively. The convergence of the combined scheme has not been proved, but simulation results show that the proposed scheme converges in a wide region around the nominal operating conditions. Simulation experiments were carried out exciting the plant with the nominal value of the base flow rate u_1 and with a multilevel random sequence added to the nominal value of the disturbance (the buffer flow rate u_2). The tuning parameters were set to $k_{u_2} = 8 \times 10^8$ and $k_x = 1000$. Figure 4*a* shows the true and estimated disturbance, where, a good agreement between them can be observed. The initial mismatch is due to the choice of initial conditions in the observer. The corresponding output is shown in Fig. 4*b*. The plot also shows how sensitive to the disturbance is the open-loop system.

The proposed observer will be used as a soft sensor to 'measure' (estimate) the disturbances in the WMPC scheme presented in Section 6.

5 Process identification

In this Section, the nonlinear white-box model (1) and (2) of the process is used to generate input-output data for the (black-box) identification of a Wiener model and a linear model of the process. The nonlinear subspace identification method of Section 3 is used to estimate a Wiener model, while the CVA subspace algorithm [20] is used for the estimation of a linear state-space model of the process.

For the purposes of identification, the model (1) and (2) was excited with band limited white noise around the nominal value of the base flow rate, keeping the buffer flow rate and the acid flow rate constant at their nominal values. The output of the system was corrupted with additive Gaussian white noise with zero mean and standard deviation $\sigma = 0.001$, in order to simulate the more realistic situation of having measurement noise.

The first 1000 data point were used for the estimation of the models, while the following 600 data points were used for validation. The estimation and validation input-output data are represented in Fig. 5.

In order to determine the model order of both the Wiener and the linear models, identification experiments were performed for ten different realisations of the measurement noise, and for model orders in the range from two to ten. The measurement noise was generated using the Matlab function `randn`, so that each time the simulation was run, a different realisation of the noise was obtained. Since it is desirable to obtain stable models for the MPC implementation, only the stability of the identified models was considered. The results are summarised in Table 2, where the letter 'S' indicates that stable models for the ten different realisations of the noise

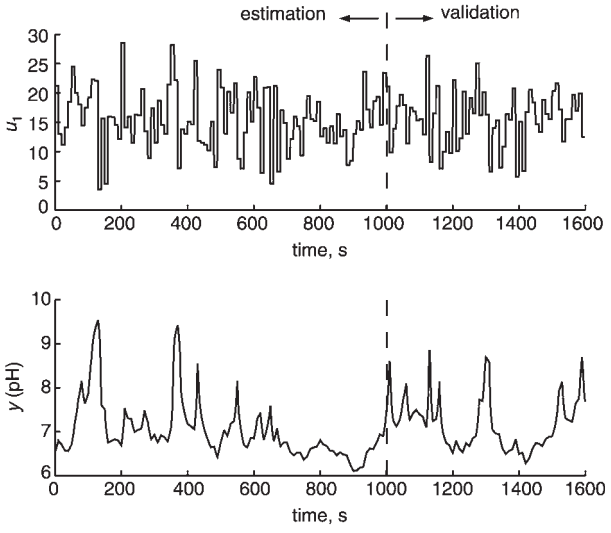

Fig. 5 *Estimation (first 1000 points) and validation (remaining 600 points) input-output data*

were obtained, while the letter 'U' indicates that at least one of the models for the ten different realisations, was unstable (actually, an average of six out of ten were unstable in these cases). The default option ('`prediction`') for the '`focus`' property of the `n4sid` algorithm in version 5 of the System Identification Toolbox for use with Matlab (hereafter referred as SIT) was employed for the first step of the nonlinear identification algorithm, as well as for the identification of the linear model. This option means that the models are determined by minimising the prediction errors, and corresponds to the optimal weighting from a statistical variance point of view [21].

Table 2 shows that it is more difficult to fit a stable linear model to the data than to fit a stable Wiener model. In this sense Wiener models perform better than linear models, since they remain stable for a wider range of model orders. Based on these results, and in order to be able to make a comparison, a model order equal to three was selected using Akaike's criterion.

The input-output data in Fig. 5 were used to identify a Wiener model using the algorithm presented in Section 3. The CVA algorithm by Larimore [20] as implemented by Ljung in SIT [27], was used in the first step of the algorithm. A third-order model, with transfer function:

$$\hat{G}(z) = \frac{0.0251z^2 - 0.0488z + 0.0237}{z^3 - 2.9210z^2 + 2.8435z - 0.9226}$$

was estimated for the linear block in the Wiener model.

On the other hand, the following third-order polynomial:

$$\hat{\boldsymbol{N}}^{-1}(yk) = 0.8918y_k^3 + 0.4065y_k^2 + 0.1988y_k$$

was estimated for the inverse of the nonlinear block in the Wiener model. The estimated nonlinear characteristic is represented in Fig. 6.

For the purposes of validation the estimated Wiener model was excited with the validation input data. The true and estimated output (for both the estimation and the

Table 2: Model order and stability

Model order	2	3	4	5	6	7	8	9	10
Wiener	S	S	S	S	S	S	S	S	S
Linear	S	S	U	U	U	U	U	U	U

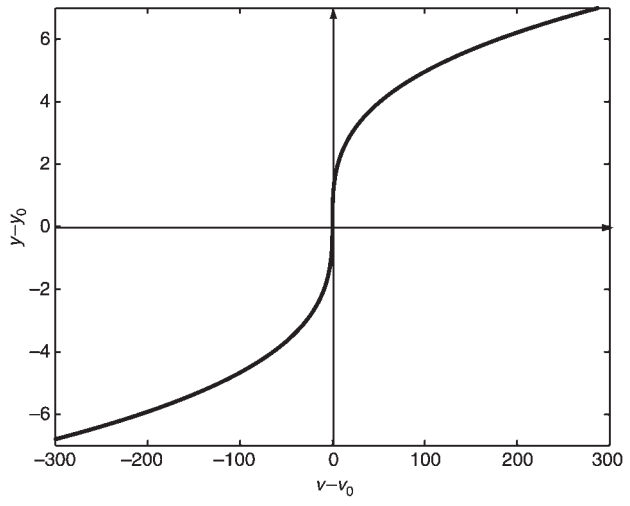

Fig. 6 *Estimated nonlinear characteristic*

validation data) are represented in Fig. 7, where a good agreement between them can be observed.

The same data were used to estimate a third-order linear model using the CVA algorithm by Larimore [20], as implemented in SIT [27]. The estimated transfer function is:

$$\hat{G}_{\text{lin}}(z) = \frac{0.0084z^2 - 0.0133z + 0.0054}{z^3 - 2.5515z^2 + 2.1610z - 0.6085}$$

For the purposes of comparison between the Wiener and the liner models, three different performance criteria were considered, namely the mean-square error (MSE), the best fit (FIT) and the variance accounted for (VAF) criterion [28].

The MSE is defined as:

$$MSE = \frac{1}{N}\sum_{k=1}^{N}(y_k - \hat{y}_k)^2$$

where y_k denotes the real output, $\hat{y}_k$ denotes the output of the model, and N denotes the number of validation data.

The best fit is defined as:

$$FIT = \left(1 - \frac{\|\boldsymbol{y} - \boldsymbol{y}_v\|}{\|\boldsymbol{y} - \boldsymbol{y}_{\text{mean}}\|}\right) \times 100$$

where $\boldsymbol{y}$ is a vector containing the output of the model when simulated with the validation input data, $\boldsymbol{y}_v$ is a vector with the validation output data and y_{mean} is the mean value of y.

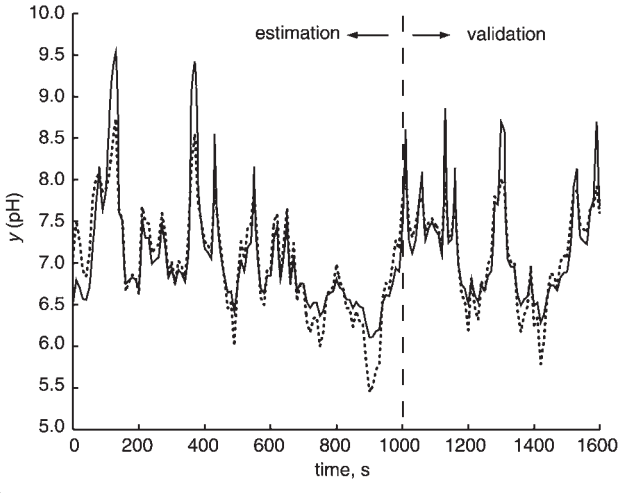

Fig. 7 *True and estimated output (estimation and validation data)*

Table 3: Error comparison between the Wiener and linear models

	MSE	FIT	VAF
Wiener	0.0728	56.8456	81.5129
Linear	0.0832	53.8870	78.7940

The variance accounted for is defined as:

$$VAF = \max\left\{1 - \frac{\text{var}\{y - \hat{y}\}}{\text{var}\{y\}}, 0\right\} \times 100\%$$

where $y = \{y_k\}_{k=1}^N$ denotes the real output sequence, $\hat{y} = \{\hat{y}_k\}_{k=1}^N$ denotes the model output sequence, and $\text{Var}\{\cdot\}$ denotes the variance of a quasi-stationary signal.

The results are summarised in Table 3. It can be seen that, for this example, the prediction capability of the Wiener model is (slightly) better than that of the linear model.

6 WMPC

In this Section, an MPC scheme based on the Wiener model is presented. The proposed WMPC scheme is used for constrained model predictive control of the pH neutralisation process using the Wiener model identified in Section 5, and its performance is compared, through simulation experiments, with that of a constrained MPC based on a linear model of the process. Also, for the purposes of comparison, a standard PID controller is implemented.

6.1 The MPC paradigm

MPC refers to a class of control algorithms in which a dynamic model of the plant is used to predict and optimise the future behaviour of the process (see the books [5] and [29] for a detailed treatment of the MPC methodology). At each control interval, the MPC algorithm computes an open-loop sequence of future moves of the manipulated variables over a control horizon M, in such a way as to optimise the future behaviour of the plant. The optimisation is performed by minimising a criterion function based on a desired output trajectory over a prediction horizon P. The first value in this optimal sequence is injected into the plant, then the horizon is displaced one step towards the future (the so-called receding horizon strategy), and the optimisation process is repeated. Typically, the criterion function is a quadratic function of the errors between the predicted output and the desired trajectory (reference) over the prediction horizon, and usually includes also terms which penalise the control effort and the rate of change of the control variable. Following the notation in [5], a typical criterion function can be written as:

$$V(k) = \sum_{i=0}^{P}\|\hat{\boldsymbol{y}}_{k+i|k} - \boldsymbol{r}_{k+i}\|^2_{\boldsymbol{Q}(i)} + \sum_{i=0}^{M-1}\|\boldsymbol{u}_{k+i|k}\|^2_{\boldsymbol{S}(i)} + \sum_{i=0}^{M-1}\|\Delta\boldsymbol{u}_{k+i|k}\|^2_{\boldsymbol{R}(i)} \quad (35)$$

where $\hat{\boldsymbol{y}}_{k+i|k}$ denotes the prediction, made at time k, of the output at time $(k+i)$, $\boldsymbol{r}_{k+i}$ denotes the value (or an estimate of it) of the reference at time $(k+i)$, and $\boldsymbol{u}_{k+i|k}$ and $\Delta\boldsymbol{u}_{k+i|k}$ denote the manipulated variable and the change of the manipulated variable, computed at time k, at time $(k+i)$. $\boldsymbol{Q}(i)$, $\boldsymbol{S}(i)$, and $\boldsymbol{R}(i)$ are positive semidefinite diagonal weighting matrices, and $\|\boldsymbol{x}\|_{\boldsymbol{W}} \triangleq \sqrt{\boldsymbol{x}^T\boldsymbol{W}\boldsymbol{x}}$ denotes the weighted 2-norm of vector $\boldsymbol{x}$. The weighting matrices $\boldsymbol{Q}(i)$, $\boldsymbol{S}(i)$ and $\boldsymbol{R}(i)$, as well as the prediction horizon P and the control

horizon M are design parameters that must be tuned to provide the controller with a satisfactory performance.

An important feature of the MPC approach is that it can deal intrinsically with constraints, which can be included in the optimisation process. In practice all processes are subject to constraints due to limited range and dynamic response of actuators, and constructive, safety, economic or environmental reasons. Usually, constraints in the magnitude of the manipulated variable, the rate of change of the manipulated variable, and the state variables and outputs, of the process are considered. The mathematical formulation of the constrained optimisation problem involved in the MPC approach can be expressed as (where the superscript i denotes the ith compoment of the corresponding vector):

$$\min_{\Delta \boldsymbol{u}}\{V(k)\} \tag{36}$$

subject to

$$\text{Process dynamics} \quad \begin{cases} \boldsymbol{x}_{k+1} = \boldsymbol{f}(\boldsymbol{x}_k, \boldsymbol{u}_k) \\ \boldsymbol{y}_k = \boldsymbol{g}(\boldsymbol{x}_k) \end{cases} \tag{37}$$

$$\text{constraints} \quad \begin{cases} u^i_{\min} \le u^i_k \le u^i_{\max} \\ \Delta u^i_{\min} \le \Delta u^i \le \Delta u^i_{\max} \\ y^i_{\min} \le y^i_k \le y^i_{\max} \end{cases} \tag{38}$$

When the criterion function $V(k)$ is quadratic (as in (35)), the constraints are linear (as in (38)), and the process model is linear, the constrained optimisation problem (36)–(38) can be written as a (QP) problem, which can be solved by resorting to standard algorithms available in the literature (a review of QP algorithms can be found in [29] Section 7.3).

6.2 The WMPC scheme

As pointed out in remark 1, an equivalent linear model for the Wiener model can be obtained by filtering the output of the process by the nonlinear basis functions used to described the inverse of the static nonlinearity. This equivalent linear model can then be used as the internal model used by a standard (i.e. based on a linear model) MPC algorithm for prediction and optimisation. As already mentioned, if the criterion is quadratic and the constraints are linear the optimisation process is a QP problem. In this way, a WMPC scheme has been introduced that retains the numerical properties of a standard MPC. The WMPC scheme is represented in, Fig. 8.

Remark 2: It is important to note that in contrast to similar approaches to WMPC in the literature (see for instance [9–11]) there is no need to invert the static nonlinearity, since it is the inverse of the nonlinearity which is delivered by the proposed identification algorithm.

Remark 3: In the proposed WMPC scheme, the optimisation no longer involves the system output $\boldsymbol{y}_k$ directly in the cost function, but the transformed (by the nonlinear basis functions used to represent the inverse of the static nonlinearity) version $\boldsymbol{Y}_k$. This would imply a suboptimal solution. However, when basis functions are used with the first element being linear (as in the considered application where polynomials are used), the system output $\boldsymbol{y}_k$ does appear directly in the cost function, while the remaining components of $\boldsymbol{Y}_k$ can be weighted to zero by an appropriate choice of the weighting matrix $\boldsymbol{Q}(i)$ in (35), resulting in an optimal solution.

6.3 Simulation results

The WMPC scheme introduced in the preceding Section was implemented using the `nlmpcsim` function in the MPC toolbox for use with Matlab [30], and the Wiener model identified in Section 5. The function allows the simulation of closed-loop systems with saturation constraints on the manipulated variables using linear models in the step format for nonlinear plants represented as Simulink S-functions. In this case, the criterion function is as in (35) but does not include the term which penalises the control effort (i.e. $\boldsymbol{S}(i) \equiv 0$ in (35)). There was no need to modify the `nlmpcsim` function for the simulation of the Wiener-model-based MPC, since the equivalent linear model described in remark 1 could be used as the internal model used by the MPC algorithm for prediction and optimisation. The closed-loop control scheme for the WMPC is represented in Fig. 8.

To take into account variations in the buffer flow rate, the nonlinear observer described in Section 4 is implemented and its output $(\hat{u}_2)$ is used as a measured disturbance by the MPC block. The combined scheme is represented in Fig. 9.

For the purposes of comparison, an MPC based on the linear model of the process identified in Section 5 was also implemented in the configuration shown in Fig. 10.

Saturation constraints in the manipulated variable are imposed to take into account the minimum and the maximum aperture of the valve regulating the base flow rate. For both cases (WMPC and linear MPC), a lower limit of 0 ml/s and an upper limit of 30 ml/s were chosen for this variable, so that the nominal operating condition is approximately in the middle of the range (the nominal value of the base flow rate being 15.55 ml/s). In both cases, the prediction horizon was chosen as $P = 20$, while the number of control moves (the control horizon) was chosen as $M = 5$. In all the simulation experiments, the system, was subjected to disturbances in the buffer flow rate as

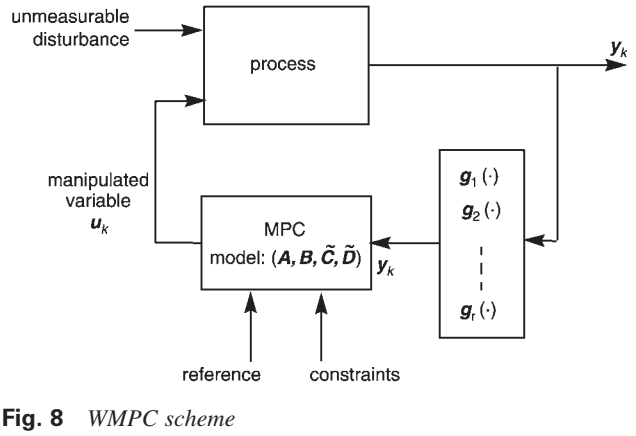

Fig. 8 *WMPC scheme*

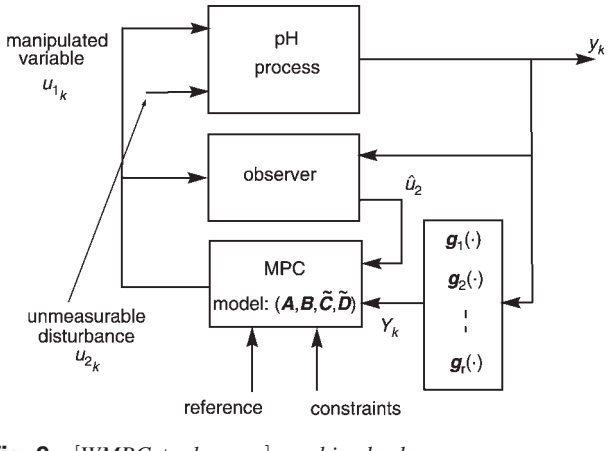

Fig. 9 *[WMPC + observer] combined scheme*

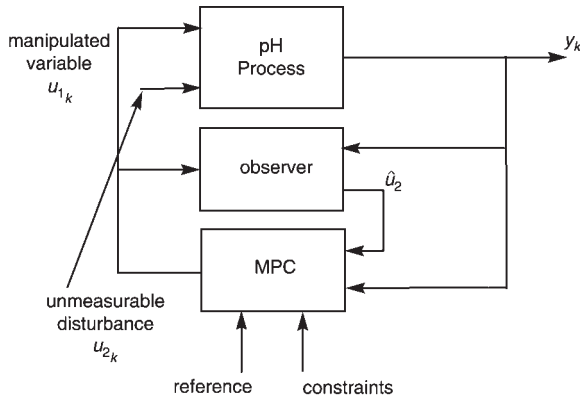

Fig. 10 *[Linear MPC + observer] combined scheme*

represented in solid-line in Fig. 4*a*, while the acid flow rate and the volume of the tank were assumed to be constant in their nominal values.

The simulation results corresponding to the linear-model-based predictive control of the process are shown in Fig. 11, while those corresponding to the Wiener-Model-Based Predictive Control are shown in Fig. 12. It can be observed that the Wiener-model-based MPC performs better than the linear-model-based one, when the operating region is far from the nominal operating conditions (i.e. pH equal to seven). The corresponding mean-squares tracking error are 0.8660 and 0.8689 for the WMPC and for the linear MPC, respectively.

For the purposes of comparison, a PID controller was implemented, and its parameters tuned using Cohen-Coon tuning rules based on the linear model of the process

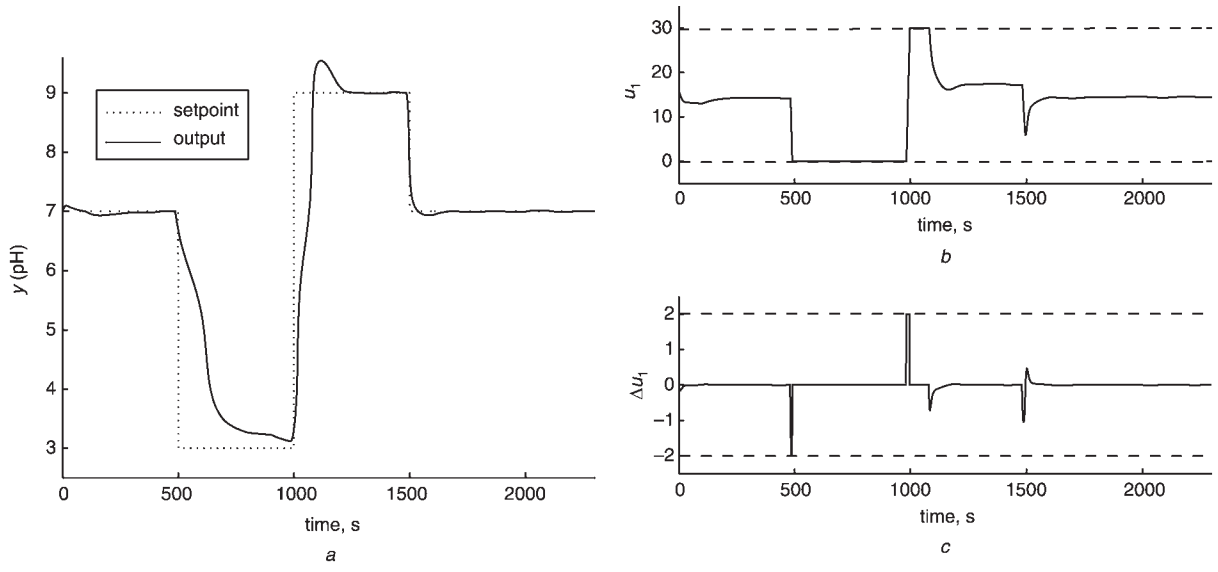

Fig. 11

a Setpoint and output with MPC based on the linear model identified in Section 5
b Manipulated variable u_1
c Rate of change of the manipulated variable Δu_1 (MSE = 0.8689)

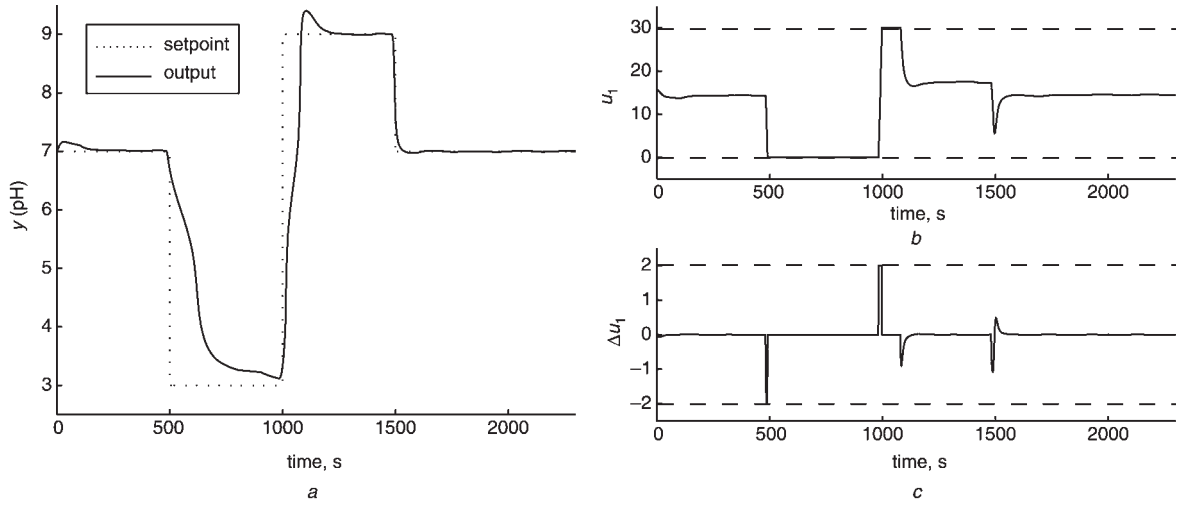

Fig. 12

a Setpoint and output with MPC based on the Wiener model identified in Section 5
b Manipulated variable u_1
c Rate of change of the manipulated variable Δu_1 (MSE = 0.8660)

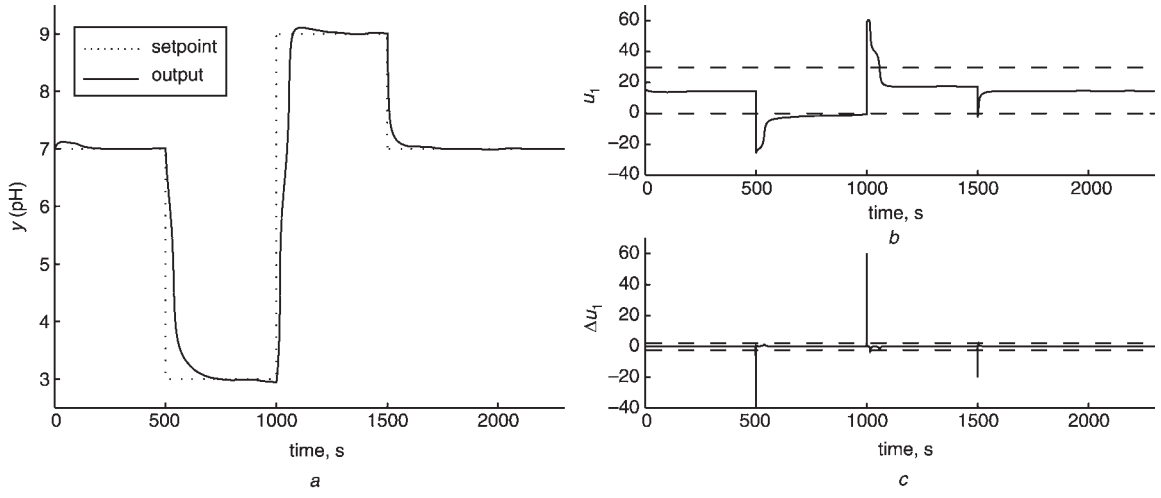

Fig. 13

a Setpoint and output with PID controller
b Manipulated variable u_1
c Rate of change of the manipulated variable Δu_1 (MSE = 0.5295)

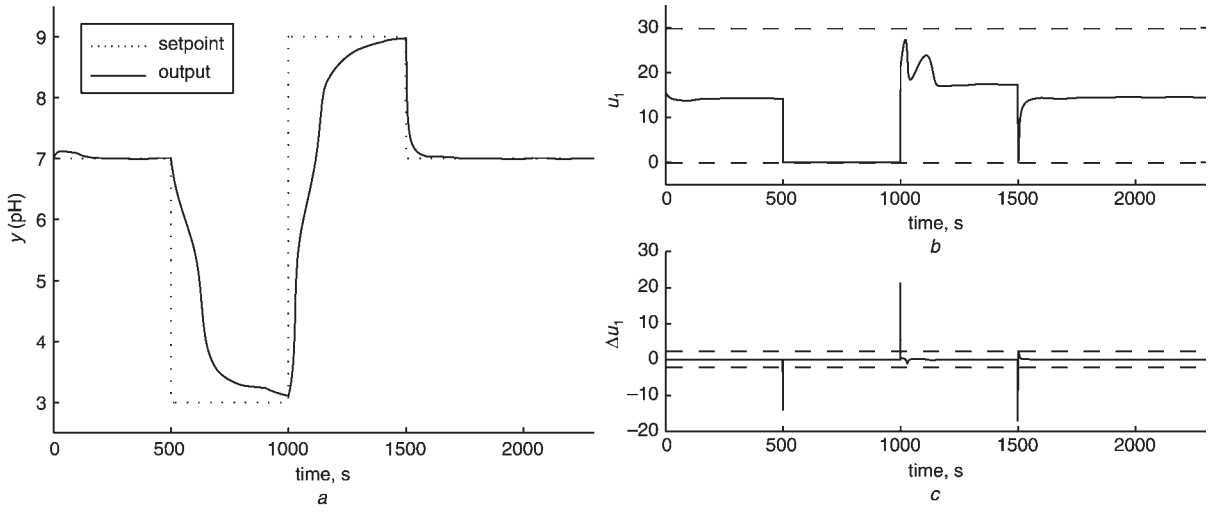

Fig. 14

a Setpoint and output with PID controller with saturation constraints
b Manipulated variable u_1
c Rate of change of the manipulated variable Δu_1 (MSE = 1.3150)

identified in Section 5. The simulation results for the case in which no constraints are imposed are shown in Fig. 13. As expected, the PID outperforms the WMPC and linear MPC controllers, but at the cost of the constraints being violated, as can be observed in the Fig. 13*b* and Fig. 13*c*. The MSE for this case is 0.5295. When saturation constraints are imposed at the output of the PID controller, its performance deteriorates considerably, as can be observed in Fig. 14*a*. In addition, the constraint on the rate of change of the manipulated variable is still being violated, as can be observed in Figs. 14*b* and 14*c*. The MSE for this case is 1.3150.

7 Conclusions

A subspace Wiener model identification and predictive control of pH neutralisation processes has been presented. Input-output data from a nonlinear, first principles simulation model of the pH neutralisation process were used for subspace-based identification of black-box linear and Wiener-type models. Simulation results showed that the identified Wiener models presented better prediction capabilities, and remained stable over a much wider range of model orders, in comparison with the identified linear models. In addition, the proposed nonlinear subspace method delivers a Wiener model in a format that can be used directly in a standard (based on a linear model) MPC strategy. The identified models were used as the internal models in an MPC of the nonlinear white-box simulation model. To take into account variations in the (unmeasurable) buffer flow rate, a nonlinear observer was introduced. Simulation results showed that, for the considered application, the WMPC outperformed the MPC based on the linear model, particularly when the system was operating away from the nominal operating conditions. The simulation results also showed that, provided there are no constraints a standard PID controller would perform adequately. However, in the presence of constraints, and due to the sensitive nature of the nonlinear process dynamics, significant degradation in the control quality would occur.

8 Acknowledgment

The first author gratefully acknowledges Dr. E. Kofman, from the Laboratory for Systems Dynamics and Signal Processing, Universidad Nacional de Rosario, for suggesting the expression for the observer gain (29).

9 References

1 Henson, M., and Seborg, D.: 'Adaptive nonlinear control of a pH neutralization process', *IEEE Trans. Control Syst. Technol.*, 1994, **2**, (3), pp. 169–182
2 Henson, M., and Seborg, D. (Eds.): 'Nonlinear process control' (Prentice Hall, NJ, 1997), Chapter 4
3 Narayanan, N., Krishnaswamy, P., and Rangaiah, G.: 'An adaptive internal model control strategy for pH neutralization', *Chem. Eng. Sci.*, 1997, **52**, (18), pp. 3067–3074
4 Wright, R., and Kravaris, C.: 'Nonlinear control of pH processes using the strong acid equivalent', *Ind. Eng. Chem. Res.*, 1991, **30**, (7), pp. 1561–1572
5 Maciejowski, J.: 'Predictive control with constraints' (Prentice Hall, NJ, 2002)
6 Henson, M.: 'Nonlinear model predictive control: current status and future directions', *Comput. Chem. Eng.*, 1998, **23**, pp. 187–202
7 Pottmann, M., and Seborg, D.: 'A nonlinear predictive control strategy based on radial basis functions models', *Comput. Chem. Eng.*, 1997, **21**, (9), pp. 965–980
8 Fruzzetti, K., Palazoglu, A., and McDonald, K.: 'Nonlinear model predictive control using Hammerstein models', *J. Process Control*, 1997, **7**, (1), pp. 31–41
9 Padwardhan, R., Lakshminarayanan, S., and Shah, S.: 'Constrained nonlinear MPC using Hammerstein and Wiener models: PLS framework', *AICHE J.*, 1998, **44**, (7), pp. 1611–1622
10 Norquay, S., Palazoglu, A., and Romagnoli, J.: 'Model predictive control based on Wiener models', *Chem. Eng. Sci.*, 1998, **53**, (1), pp. 75–84
11 Norquay, S., Palazoglu, A., and Romagnoli, J.: 'Application of Wiener Model Predictive Control (WMPC) to a pH neutralization experiment', *IEEE Trans. Control Syst. Technol.*, 1999, **7**, (4), pp. 437–445
12 Kalafatis, A., Arifin, N., Wang, L., and Cluett, W.: 'A new approach to the identification of pH processes based on the Wiener model', *Chem. Eng. Sci.*, 1995, **50**, (23), pp. 3693–3701
13 Boyd, S., and Chua, L.: 'Fading memory and the problem of approximating nonlinear operators with Volterra series', *IEEE Trans. Circuits Syst.*, 1985, **32**, (11), pp. 1150–1161
14 Bloemen, H., Chou, C., van den Boom, T., Verdult, V., Verhaegen, M., and Backx, T.: 'Wiener model identification and predictive control for dual composition control of a distillation column', *J. Process Control*, 2001, **11**, pp. 601–620
15 Greblicki, W.: 'Nonparametric identification of Wiener systems by orthogonal series', *IEEE Trans. Autom. Control*, 1994, **39**, (10), pp. 2077–2086
16 Wigren, T.: 'Recursive prediction error identification using the nonlinear Wiener model', *Automatica*, 1993, **29**, (4), pp. 1011–1025
17 Billings, S., and Fakhouri, S.: 'Identification of systems containing linear dynamic and static nonlinear elements', *Automatica*, 1982, **18**, (1), pp. 15–26
18 Van Overschee, P., and de Moor, B.: 'N4SID: Subspace algorithms for the identification of combined deterministic-stochastic systems', *Automatica*, 1994, **30**, (1), pp. 75–93
19 Verhaegen, M.: 'Identification of the deterministic part of MIMO state space models given in innovations form from input-out data', *Automatica*, 1994, **30**, (1), pp. 61–74
20 Larimore, W.: 'Canonical variate analysis in identification, filtering, and adaptive control'. Proc. 29th IEEE Conf. on Decision and Control, Honolulu, HI, December 1990, pp. 596–604
21 Westwick, D., and Verhaegen, M.: 'Identifying MIMO Wiener systems using subspec model identification methods', *Signal Process.*, 1996, **52**, pp. 235–258
22 Verhaegen, M., and Westwick, D.: 'Identifying MIMO Hammerstein systems in the context of subspace model identification methods', *Int. J. Control*, 1996, **63**, (2), pp. 331–349
23 Gómez, J.C., and Baeyens, E.: 'Subspace identification of multivarial Hammerstein and Wiener models'. Proc. 15th International Federation of Automatic Control World Congress, Barcelona, Spain, July 2002, pp. 2849–2854
24 Friedland, B.: 'A nonlinear observer for estimating parameters, in dynamic systems', *Automatica*, 1997, **33**, (8), pp. 1525–1530
25 Sastry, S., and Bodson, M.: 'Adaptive control - stability convergence and robustness' (Prentice Hall, NJ, 1989)
26 Isidori, A.: 'Nonlinear control systems' (Springer, Berlin, 1995, 3rd edn.)
27 Ljung, L.: 'System identification: toolbar, user's guide, ver. 5' (The MathWorks, Inc., Natick, MA, 2000)
28 Ljung, L.: 'System identification: theory for the user' (Prentice Hall, Englewood Cliffs, NJ, 1999, 2nd edn.)
29 Camacho, E., and Bordons, C.: 'Model predictive control' (Springer, Berlin, 1999)
30 Morari, M., and Ricker, N.: 'Model predictive control toolbox-for use with Matlab, user's guide' (The MathWorks, Inc., Natick, MA, 1994)

10 Appendix

Proof of error convergence: The estimation error dynamics are given by (23), that is:

$$\dot{\boldsymbol{e}} = -\boldsymbol{L}(\boldsymbol{x})e \tag{39}$$

Let the candidate Lyapunov function be $V(e) = e^2$, and let $\boldsymbol{L}(\boldsymbol{x})$ be a positive semidefinite symmetric matrix. Then, the orbital derivative of $V(e)$ is given by:

$$\frac{dV}{dt} = \frac{\partial V}{\partial e}\dot{\boldsymbol{e}} = -\boldsymbol{L}(\boldsymbol{x})e^2 \leq 0 \tag{40}$$

which is decreasing along the trajectories solution of (39) This proves that $e \in L_2 \cap L_\infty$. Resorting to Barbalat's lemma (see lemma 1.2.1 and corollary 1.2.2 in [25]), a sufficient condition for the error to converge to zero is that e is uniformly continuous, or equivalently that $\dot{\boldsymbol{e}}$ is bounded $(\dot{\boldsymbol{e}} \in L_\infty)$. Since e is bounded, the condition $\dot{\boldsymbol{e}} \in L_\infty$ is guaranteed if $\boldsymbol{L}(\boldsymbol{x})$ is bounded, which concludes the proof. □